

# FIELD TEST ON THE COOPERATION OF NSM STRENGTHENING AND EXTERNAL TENDON RETROFITTING TECHNIQUE

*Jianxi Yang, Jiaping Yu, Quansheng Sun, Hongshuai Gao and Jiawei Wang*

*Department of Civil Engineering, Northeast Forestry University, Harbin, 150040, China; yangjianxi@nefu.edu.cn, yujaping@hotmail.com, hrbsqs@126.com, ghsphd@126.com, wjw526@126.com*

## ABSTRACT

In this paper, post-tension and steel plate near-surface mounted (NSM) strengthening systems are proposed to strengthen deteriorated and cracked large box girder rigid frame bridge without altering appearance and dimension of the bridge. The reinforcement method mainly improves the bearing capacity through external prestressed tendons, and bonding steel plate can enhance the shear resistance of the bridge. The main purpose is to study the structural mechanical properties before and after the reinforcement of rigid frame bridges. Take a 540m rigid frame box girder bridge as an example. The static load test of the bridge before and after reinforcement is carried out. The deflection and strain of the middle cross section of the span are measured in the static test. A finite element analysis model was also developed and verified static loading test data. The results show that structural bearing capacity and performance of the bridge were enhanced with the post-tension and NSM strengthening systems cooperatively.

## KEYWORDS

Static loading test, Finite element method, NSM strengthening, Prestressed concrete rigid frame bridge, External tendon retrofitting technique

## INTRODUCTION

With the development of China's economy, growing traffic volumes pose a threat on the bearing capacity of existed traffic system, especially those in-service highway bridges designed according to the old code no longer meet the requirements of use. In the course of bridge operation, it is also found that the prestressed concrete continuous box girder bridge has the problems of beam cracking and excessive mid-span deflection [1-2].

Many researchers have studied proper repair and strengthening methods to solve the problems that occur in concrete bridges. Heeyoung et al [3] studied the structural behavior of an old 12.5m reinforced concrete T type bridge before and after using post-tension NSM strengthening systems, and verified it by finite element model calculation. The results show that the post-tensioned NSM reinforcement system can improve the bridge bearing capacity and performance of the bridge. Osman et al [4] applied fiber-reinforced polymer (FRP) composite laminates to strengthen an aging reinforced concrete T-beam bridge, the results of static load test and finite element analysis before and after reinforcement revealed that main rebar stresses were moderately reduced, concrete stresses (flexural and shear) moderately increased, and transverse live-load distribution to the beams slightly improved under service load after strengthening. Zhang [5] presents the experimental response of reinforced concrete T-beams strengthened with a

composite of prestressed steel wire ropes embedded in polyurethane cement. The experimental study on reinforcement shows that the reinforcement technique has potential as an external strengthening technique for concrete structures. Morris [6] investigated the durability of bonded and unbonded prestress tendons. Xu [7] used analytic hierarchy process (AHP) to establish the quality evaluation system of prestressed reinforcement system, and verified the evaluation system rationally in combination with practical engineering. Shen [8] presented the design and reasonable arrangement of external prestressed tendons for multi-span curved box girder bridges. Ibrahim [9] studied the bending mechanical properties of prestressed continuous concrete beams through experiments and verified them by finite element method(FEM). The ultimate bearing capacity can be improved by increasing the effective depth. In recent years, the application of bonded steel reinforced polymer(SRP) [10], carbon fiber reinforced polymer (CFRP) sheets [11-13], ultra high performance fiber reinforced concrete (UHPFRC)[14], post-tension near-surface-mounted strengthening systems and external post-tensioning reinforcement techniques has become more and more extensive and achieved good reinforcement effect in concrete beam bridge and box girder Bridge [15-20].

However, ignoring the prominent defects of bridges or lacking real judgment on the existing disease assessment will not only affect the normal use of the structure, but also pose a potential threat to the social environment and safety. In view of this, it is very important to analyze the disease of prestressed concrete continuous rigid frame bridge and select effective reinforcement measures according to the concrete conditions. Bridge reinforcement not only serve to improve the bearing capacity and stiffness of the bridge, but also need to consider factors such as aesthetic, material saving, construction difficulty.

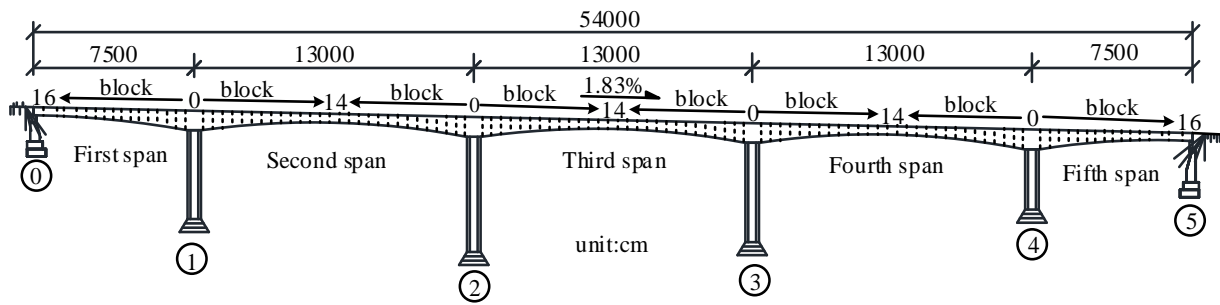
In order to study the performance of the strengthening technique, structural behaviors were compared before and after external tendon and steel plate strengthening of prestressed concrete rigid frame bridge. Furthermore, the experimental results were investigated with those of a proposed finite element analysis model. Finally, the strengthening performance was analyzed using finite element analysis.

## BACKGROUND

### Description of the bridge structure

The prestressed concrete bridge is a continuous segmental box girder T-shape rigid frame bridge that is located in Hegang-Dalian Highway within the Heilongjiang Province of north-east China. The bridge is 540-m long and 12-m wide. The transverse arrangement of bridge deck is 0.5m (anti-collision railing) +11.0m(lane)+0.5m (anti-collision railing). Span arrangement is 75m+3×130m+75m. The longitudinal slope and unidirectional transverse slope of bridge deck is 1.83% and 2.0%, respectively. The superstructure consists of 5-span continuous prestressed concrete rigid frame large box girder. The box girder is of single box single chamber structure, the height of segment No.0, which is on the top of the pier, is 7.0m, whereas the height of box girder is 2.5m at mid-span of the bridge. The height of longitudinal bridge box girder varies according to the equation  $y=0.0026724x^{1.8}$ . Bottom plate of the box girder is 5.6m in width, and the flange of the bridge is 3.2m in width. The longitudinal and transverse prestressed tendons adopts  $\phi^{15.24}$  low relaxation high strength steel strand of 270 grade in accordance with the standard ASTM.A416-90a, each longitudinal prestressed tendon is composed of 15 prestressed steel strands, and the tension control force is 2932.9kN. Each transverse prestressed tendon is composed of 3 prestressed steel strands, and the tension control force is 782.1kN. The arrangement spacing of the transverse prestressed tendon is 80 cm. The substructure is composed of double-thin-walled piers, ribbed plate type abutment, and solid expanding foundation. Piers are 5.6m wide in transverse direction, and 1.2m wide in longitudinal direction with spacing of 3.6m. The heights of

the piers are 35m, 45m and 24m, respectively. The design load of bridge reinforcement is highway grade I [21] (the original design load is vehicle super-20, trailer-120). The bridge was opened to traffic in 2006 and strengthened in 2016. Figure 1(a) shows the elevation drawing of the bridge structure, Figure 1(b) shows the overall perspective of the strengthening bridge.



(a)



(b)

Fig.1 – Details of the strengthening bridge: (a) elevation drawing; (b) overall perspective

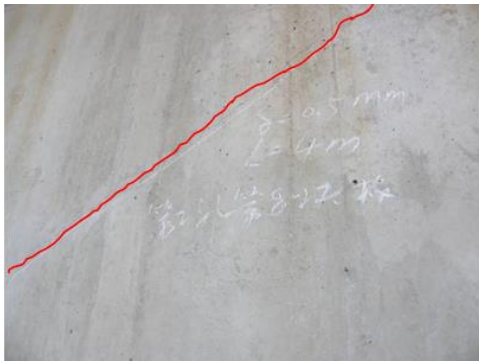
## Bridge diseases

The rigid frame continuous box girder bridge in this study was first open to traffic in 2006. However, after as little as 6 years of operation, the degradation of material properties and load bearing capacity of bridge appeared. During routine inspection in 2012, 2013 and 2015, cracks were observed on the top slab, web and bottom slab, more severe on the exterior surfaces than the interior of box girder. Length, width and number of cracks were growing as time goes on. Most of the cracks were between 0.15mm ~ 0.4mm in width and 0.3m ~ 7m in length. According to the codes and specifications that prestressed concrete beams are not allowed to have cross-sectional cracks, and the allowable width of longitudinal cracks is 0.2mm. The width of some longitudinal cracks on the box girder exceeds the specified value.

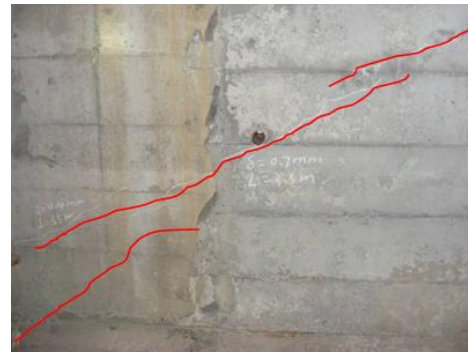
In the routine inspection of the bridge in 2012, bridge detection results show that there was a large number of oblique cracks in the outside of the web of box girder near the fulcrum of the second span and closure segment (block 6-14) of the third span. The crack width is generally between 0.2~0.5mm and roughly distributed in the direction of  $20^{\circ} \sim 45^{\circ}$ , and the maximum crack width is 0.5 mm. These cracks show the characteristics of obvious stress cracking of the principal tensile stress. There are about 21 oblique cracks in the outside of the web of box girder, the total length of the oblique cracks is about 70.7m, the total length of the left oblique cracks is 29.5m, and

the total length of the right oblique cracks is 41.2m. The cracks are roughly distributed in the 130m main span.

Routine inspection of the bridge was conducted again in 2013 and 2015, respectively. Cracks distribution of box girder was similar compared to 2012 inspection. However, cracks on the web gradually developed into transverse cracks at the chamfering angle of the top slab of box girder. As a result, there were 156 oblique cracks detected on the web of the box girder, the crack total length was 38.6m, among which 72 cracks on the right side with a total length of 19.3m and 84 cracks on the left side with a total length of 19.3m. There were about 38 cracks on the exterior surface of the web with a total length of about 11.95m, among which 11 cracks on the left side with a total length of 32.9m, and 27 cracks on the right side with a total length of 86.6m. Crack distribution on the web of the box girder is shown in Figure 2. In the following figures, L represents the length of the crack,  $\delta$  represents the width of the crack, and  $\alpha$  indicates the angle between the crack and the longitudinal bridge direction.



(a) No. 8 block exterior surface oblique crack (L=4m  $\delta$ =0.5mm  $\alpha$ =45°)



(b) No. 8 block interior surface oblique crack (L=8m  $\delta$ =0.7mm  $\alpha$ =35°)



(c) No. 10 block right side interior surface oblique crack (L=9m  $\delta$ =0.5mm  $\alpha$ =35°)



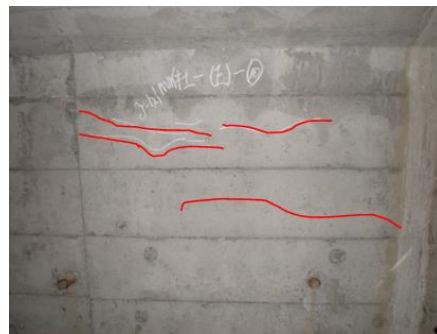
(d) No. 11 block left side interior surface crack (L=3.4m  $\delta$ =0.15mm  $\alpha$ =30°)



(e) No. 13 block right side interior surface crack (L=6.7m δ=0.15mm α=45°)



(f) No. 10 block left side interior surface crack (L=2.9m δ=0.10mm α=45°)



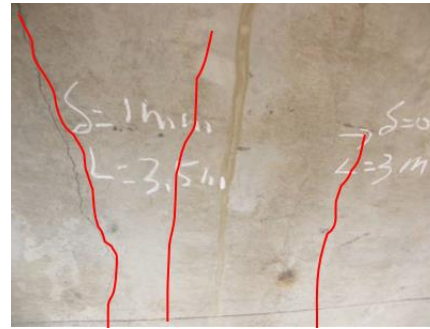
(g) No. 14 block right side interior surface crack (L=2.4m δ=0.10mm α=15°)

*Fig.2 – Crack distribution on the web of box girder of the second span*

In 2013 inspection, 5 longitudinal cracks were observed at the exterior surface of box girder bottom slab of closure segment of the second span, the length of cracks were ranging from 2m to 7m and the width of cracks were ranging from 0.6mm to 4mm. In 2015 inspection, it was found that there were 9 longitudinal cracks on the bottom slab of the closure segment. There were 3 longitudinal cracks on the bottom slab of closure segment of the third span and 7 longitudinal cracks in closure segment of the fourth span, whereas bottom slab of second span was the most severe, the maximum width of the longitudinal crack is up to 4 mm and crack bulge deformation is about 3 mm. After chipping away loose concrete around the crack, hollow section was found and corrugate pipe was slightly damaged. Cracks on the bottom slab of the box girder of closure segment of second span and third span are shown in Figure 3.



(a) bottom slab cracks of second span  
(L=20.5m δ=0.6mm)



(b) bottom slab cracks of third span  
(L=8.5m δ=0.7mm)



(c) longitudinal bottom crack of second span (L=0.7m δ=4mm)



(d) Longitudinal crack hollow section of second span



(e) Longitudinal crack hollow section of second span



(f) longitudinal crack corrugate pipe deterioration of second span

*Fig. 3– Cracks on the bottom slab of the box girder of closure segment*

Moreover, there is a vertical crack on interior diaphragm of box girder end of the first span. The width and length of the crack are 0.25mm and 200cm, respectively, as shown in Figure 4.



Fig. 4 – Crack on interior diaphragm of box girder end of the first span  
( $L=2m$   $\delta=0.25mm$ )

The number, length and width of cracks increase with the number of years of operation as shown in Figure 5. From 2012 to 2013, the width of cracks on the web of box girder increased by 24.77%, the number of cracks increased by 103, and the length increased by 229.37m. From 2013 to 2015, the width of cracks increased by 11.26%, the number of cracks increased by 60, and the length increased by 163.03m. The main causes of the development of the bridge crack in the period from 2012 to 2015 is that the increase of the heavy-load vehicle exceeds the design load capacity of the bridge, leading to the main tensile stress generated by the live load exceeding the design value, and the box girder generates the oblique crack disease.

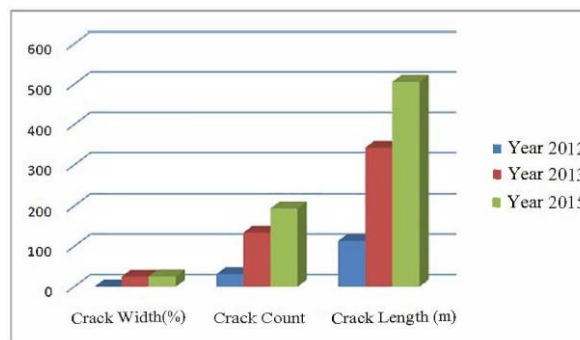


Fig. 5 – Comparative Diagram of cracks in Box girder in different Detection years

### External Tendon and Steel Plate Strengthening

The external tendons were stretched at both ends. External prestressing tendons were cross-anchored at the top of the main pier, and the cast-in-place anchor block was used for anchoring at the box girder end. The number of external prestress tendons is determined by reducing the web shear force and making the main tensile stress of the web of the box girder meet the code, and increasing the bending capacity of the normal section of the span and the compressive stress reserve at the bottom of the beam. Eight bundles of 17  $\phi^s$  15.24 prestressed steel strands are used in each span, and the tensile control stress is 930MPa, which is 50% of the standard strength. The detailed arrangement of external prestressed tendons is shown in Figure 6.

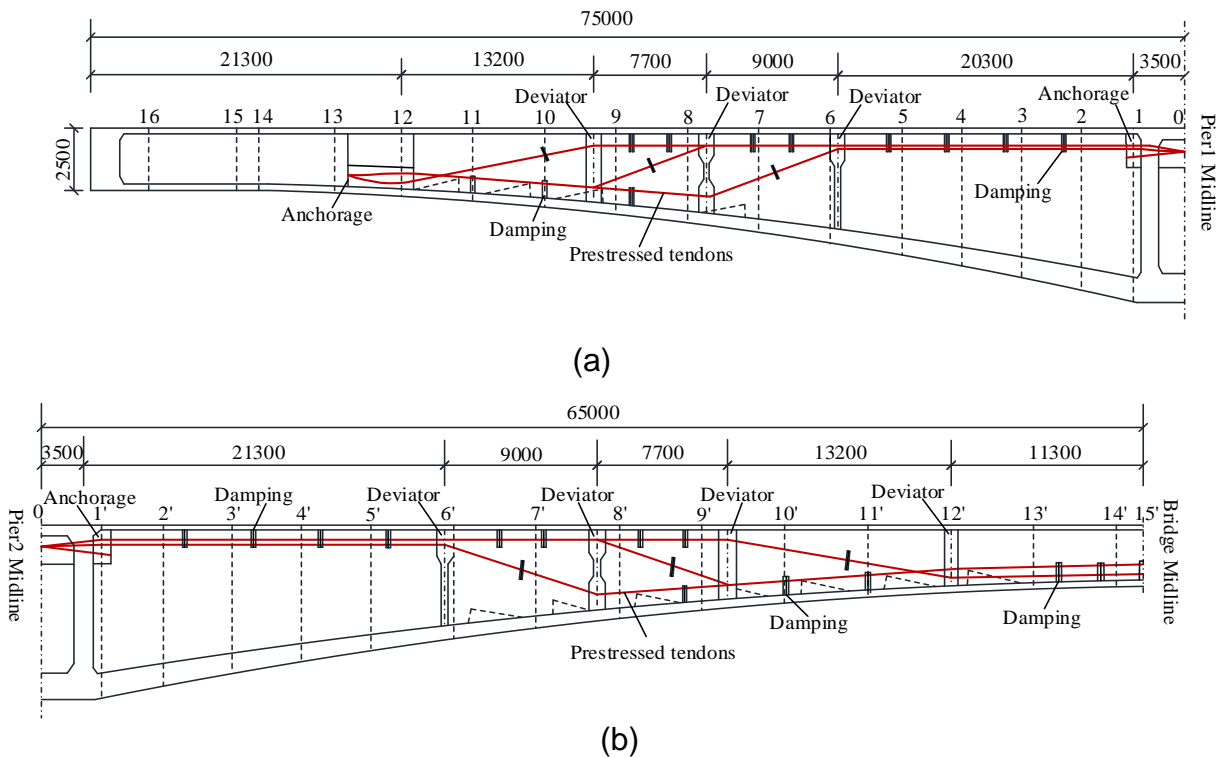
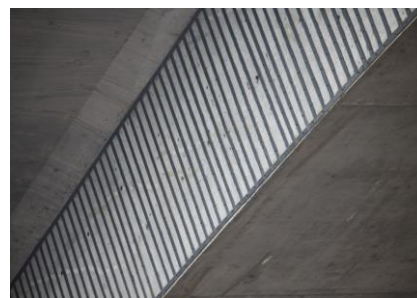


Fig. 6 – External prestressing strands arrangements for: (a) side span; (b) middle span (unit: mm)

The vertical steel strip is pasted on both sides of the web to strengthen the oblique section of the box girder. The reinforcement range of the inside of the web of the box girder is from 6 to 14 girder segments, and that of the outer side of the web is from NO.6 to NO.10 block of the middle span. The steel reinforcement of the top plate of box girder is the non-thickened area of the web. The bending capacity of the bottom plate is increased in the range of 15 m of the mid-span closure section by the use of an adhesive steel strip. The penetration anchoring is carried out by anchoring bolt in the range where is no bottom plate prestress in the center of web and bottom plate. The thickness and width of the steel plate are 6mm and 60mm, respectively. The length of the steel plate depends on the disease distribution area. The steel plate is made of Q235 steel. The thickness of zinc-rich primer is 70 μ m, and the epoxy asphalt paint consists of intermediate layer and topcoat, with a total thickness of 200 μ m. Steel plate reinforcement of box girder is shown in Figure 7.



(a)



(b)



(c)

(d)

*Fig.7 – Steel plate reinforcement of box girder: (a) inner wall of web (b) outer wall of web (c) and (d) bottom plate*

## EXPERIMENTAL PROGRAM

The design load grade of deteriorated rigid frame continuous box girder bridge was vehicle-20, trailer-100 according to Chinese design code JTG 021-1985[22]. The lane load is composed of the uniform load of 10.5kN/m and the concentrated load of 360kN, which is similar to AASHTO HS15 loading in the American bridge design code[23]. Static loading tests were performed to obtain structural behaviour of the bridge before and after strengthening (Figure 8). The main objectives of the static loading test were to test the following:

1. Strain in the static load test in the vicinity of the supporting point;
2. Strain of the most unfavourable section of side span and middle span under static load test;
3. Deflection of the most unfavourable section of side span and middle span under static load test.



a)



b)

*Fig.8 – Illustration of field static load test (a) eccentric loading test before or after strengthening; (b) centric loading test before or after strengthening*

## Loading test truck arrangement

A total of 16 triaxial trucks were used in static loading test. Trucks #1~#8 were used before strengthening and trucks #9~#16 were used after strengthening. The sum of axle load and axle load of truck is shown in Table 1.

Tab. 1 - Characteristics of the loading truck (kN)

Truck	Front axle	Middle axle	Rear axle	Total axle load
#1	73.1	148.1	144.1	365.3
#2	73.2	147.5	145.5	366.2
#3	73.9	148.8	146.8	369.4
#4	73.4	147.8	145.8	367.0
#5	73.5	145.0	149.0	367.5
#6	73.5	149.1	145.1	367.7
#7	74.1	148.2	148.2	370.5
#8	73.1	147.3	145.3	365.7
#9	74.1	147.1	149.1	370.3
#10	73.8	149.7	145.7	369.2
#11	74.4	149.7	147.7	371.8
#12	73.3	147.6	145.6	366.4
#13	73.7	148.3	146.3	368.3
#14	74.2	148.3	148.3	370.8
#15	73.9	147.9	147.9	369.7
#16	73.6	148.2	146.2	368.0

Centric and eccentric loading were performed on mid-span cross-sections and eccentric loading was performed on pier cross-section, maximum bending moments were measured for each load cases before and after strengthening. Static Loading Schemes are shown in Table 2. Eccentric and centric loading location drawing plans are shown in Figure 9.

Tab. 2 - Static Loading Scheme

Case No.	Location	Loading condition	Deflection	Strain Gauges
1	midspan of first span	centric	√	√
2	midspan of first span	eccentric	√	√
3	midspan of second span	centric	√	√
4	midspan of second span	eccentric	√	√
5	pier 2	eccentric	---	√
6	midspan of third span	centric	√	√
7	midspan of third span	eccentric	√	√

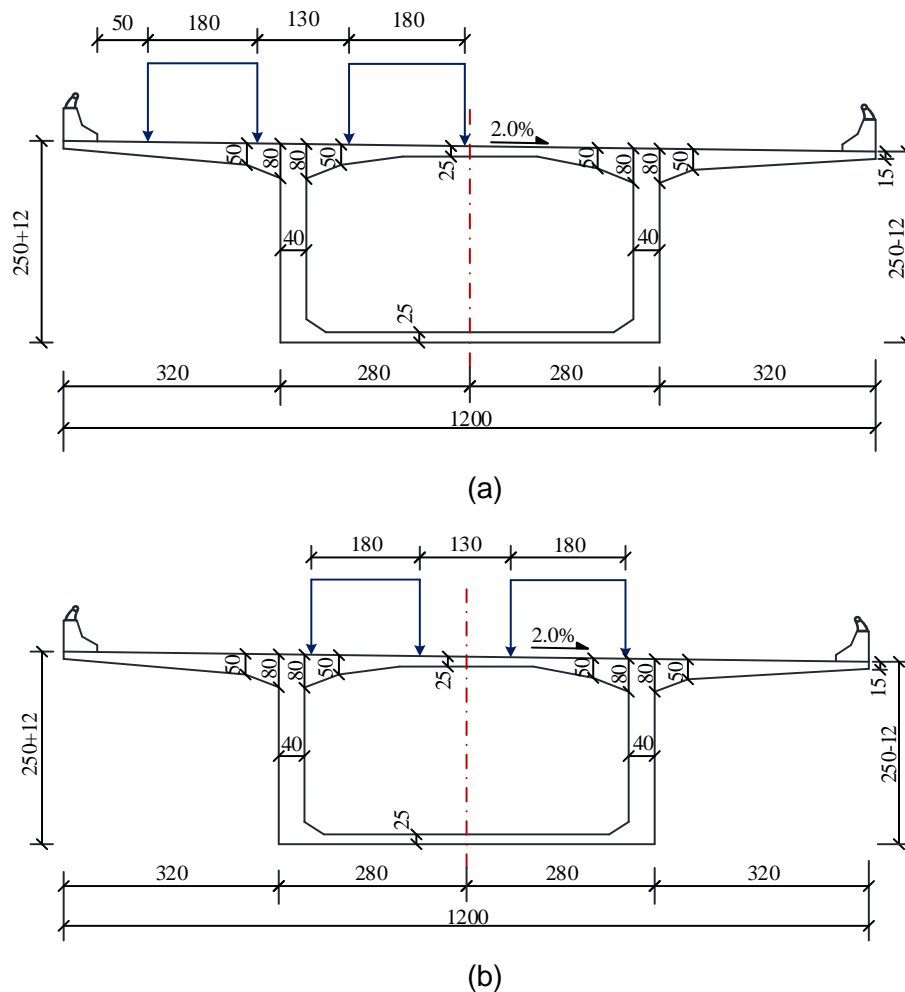


Fig. 9 –Lateral arrangement of static load test load (a) eccentric loading; (b) centric loading (unit: cm)

### Deflection measuring point and strain sensor layout

The bridge detection system consists of deflection measuring point and strain sensors. Deflection measuring point and strain sensors were strictly controlled at the same locations before and after strengthening. Deflection measuring points were placed at the middle of the span, the measuring point number is d1, d2 and d3. The deflection is measured by precision level. Strain measuring points of midspan were placed on the interior surface of the top slab, web and bottom slab of the box girder, the measuring point number is s1~s11. Strain measuring points of pier cross-section were placed only on the inner wall of top slab and web of box girder, the measuring point number is ps1~ps7. The strain sensors are all vibrating wire strain meters. Deflection measuring point and strain sensor layout of box girder before and after the strengthening are shown in Figure10.

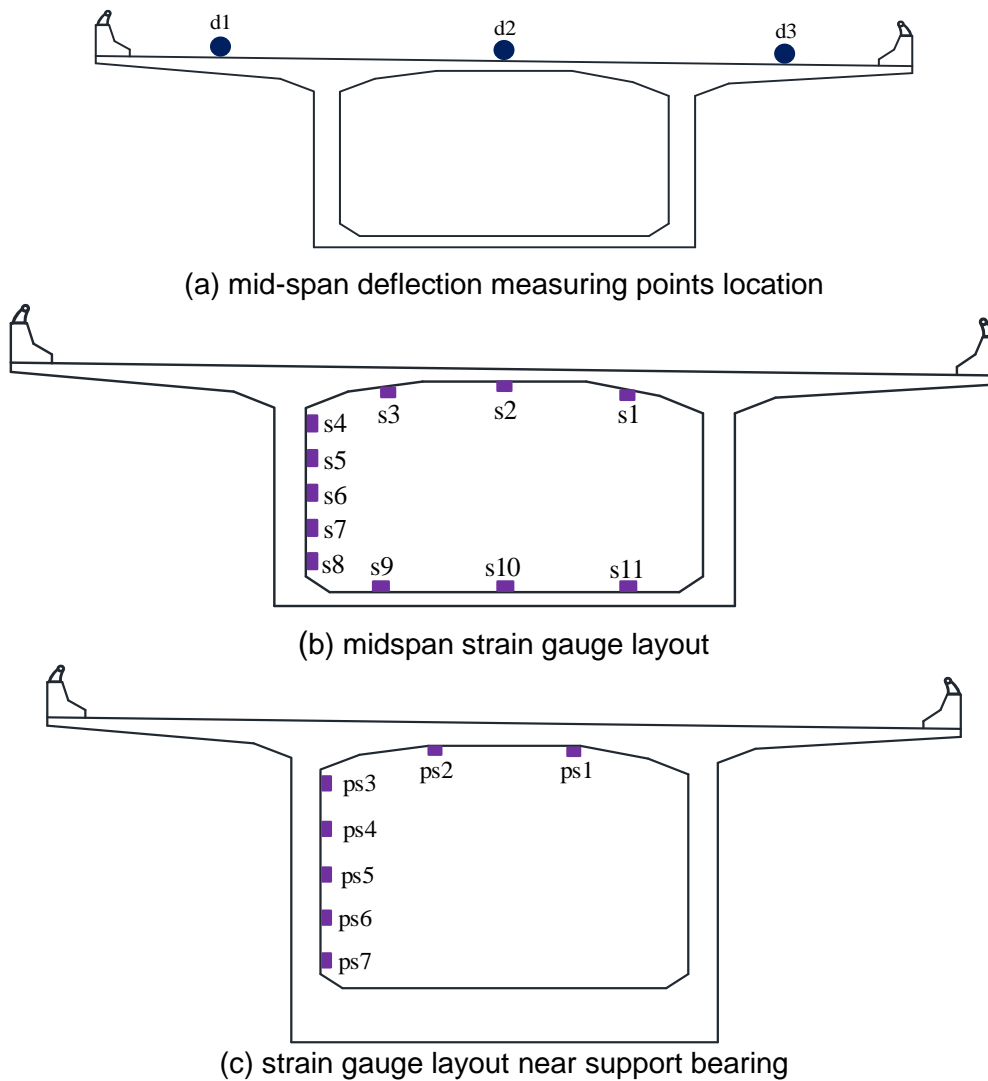


Fig. 10 – Deflection measuring point and strain sensor layout of box girder

## ESTABLISHMENT OF FINITE ELEMENT MODEL

The Midas Civil software is used to establish the spatial finite element model of bridge before and after reinforcement, as shown in Figure 11. The box girder and pier are simulated by beam element. The prestressed steel wire strand bundle number of top plate, bottom plate and the web of box girder of the bridge is 229,100 and 64, respectively. Eight bundles of 17  $\varphi^{s15.24}$  prestressed steel strands are used in each span of the bridge after reinforcement. The prestressed steel wire strand bundles are simulated by tension frame unit. There are 290 units in the bridge finite element model. The connection between the top of the pier and the box girder is rigid connection, and the bottom of the pier is consolidation connection. The end of the bridge constrains vertical displacement and lateral displacement. The load of the vehicle of static load test is simplified into a concentrated force calculation, the actual bearing capacity of the reinforced bridge is obtained by comparing the calculated value with the measured value.

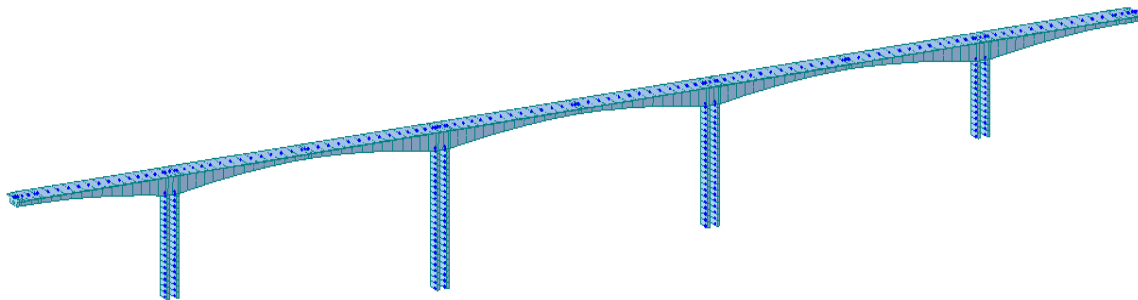
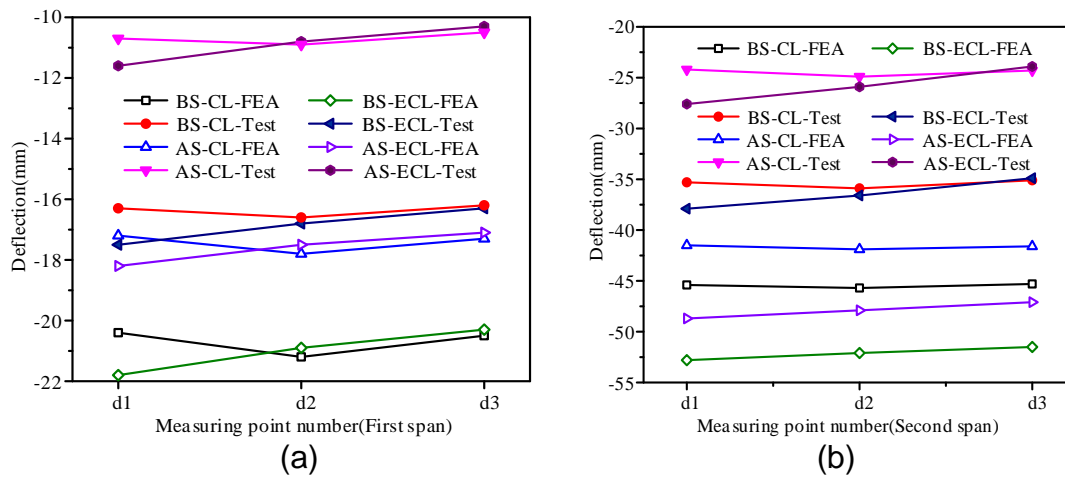


Fig. 11- Spatial finite element model of bridge

## RESULTS & DISCUSSION

### Deflection

The deflection value, as the key control parameter of the static load test of the bridge, reflects the overall stiffness of the bridge structure. The finite element model calculation value and test value for load test of deflection before and after strengthening are shown in Figure 12. In the following figures, BS and AS indicate before and after strengthening, CL and ECL indicate centric and eccentric load, FEA and Test indicates finite element analysis and static load test result, respectively.



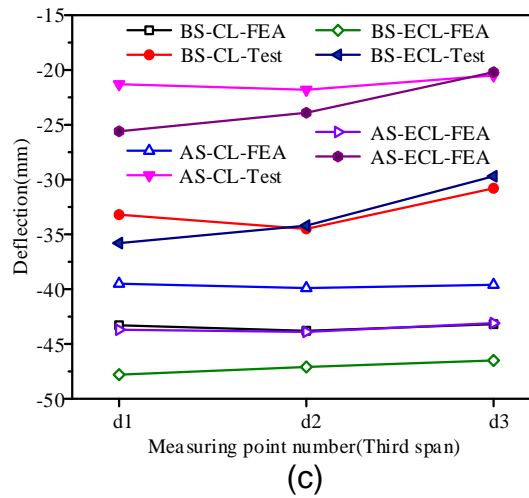


Fig.12– Calculated and Measured vertical displacement curve for (a) First span; (b) Second span; and (c) Third span

After bridge reinforcement, as shown in Figure 12, under the action of load test under each working condition, the measured deflection values of each measuring point are less than the theoretical values. For the first span, the deflection coefficient of correction is between 0.60 and 0.64, the coefficient of correction of the bridge is increased by 22.7% after reinforcement, the bearing capacity has increased by 18.2%. For the second span, the deflection coefficient of correction is between 0.51 and 0.59, the coefficient of correction of the bridge is increased by 23.8% after reinforcement, the bearing capacity has increased by 17.5%. For the third span, the deflection coefficient of correction is between 0.47 and 0.59, the coefficient of correction of the bridge is increased by 27.0% after reinforcement, the bearing capacity increased by 19.7%. The results show that external prestressing strengthening can significantly improve the performance of the structure. However, due to the loss of prestress caused by reinforcement construction, the actual deflection improvement value is less than the theoretical deflection improvement value.

Measured deflection values of the bridge after reinforcement are all smaller than the values of the bridge before reinforcement. The maximum displacement after the strengthening decreased to 27.6mm, compared to 37.9mm before strengthening. After strengthening, the displacement of all spans decreased. The strengthening effect of the maximum displacement of the static loading test was improved by 27%.

### Strain

Strain is another key data that reflects the stress of bridge. Measured strain data under static loading before and after strengthening is shown in Figure13 and Figure14.

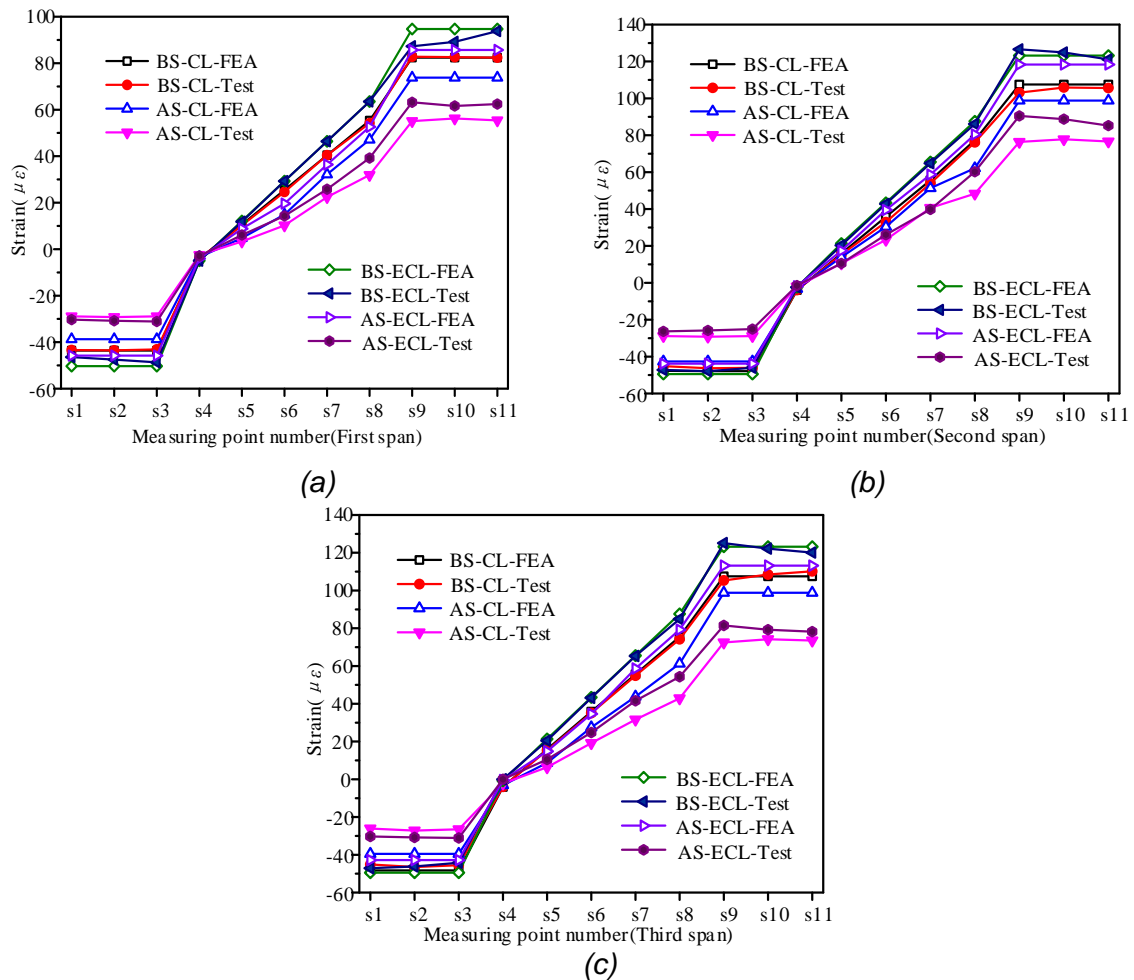


Fig. 13 – Measured strain data under static loading tests

After bridge reinforcement, as shown in Figure 13, the measured strain values of each measuring point are less than the theoretical values of finite element model. The measured strain values of each load cases of the first span all show improvement after external prestressing strengthening. For the first span, the strain coefficient of correction is between 0.66 and 0.75, which indicated stiffness improvement of the bridge structure. The average increment of load carrying capacity and coefficient of correction are 28% and 27%, respectively. For the second span, the strain coefficient of correction is between 0.57 and 0.79. The average increment of load carrying capacity and coefficient of correction are 26% and 27%, respectively. For the third span, the strain coefficient of correction is between 0.57 and 0.76. The average increment on strain and coefficient of correction of midspan centric loading are all 27%, and the average increment on strain and coefficient of correction of midspan eccentric loading are 23% and 24%, respectively.

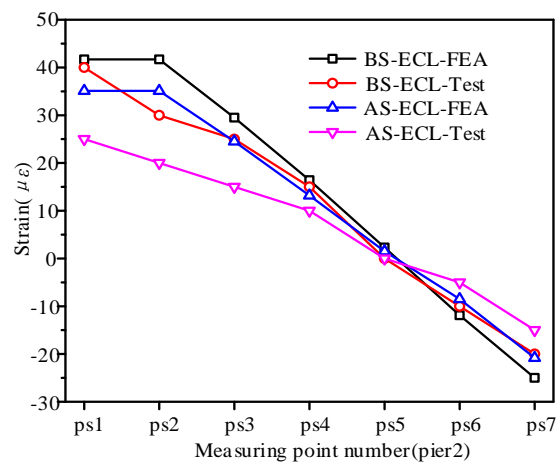


Fig. 14 – Measured strain data under static loading tests of pier 2

At pier 2, as shown in Figure 14, the measured strain values of each measuring point are less than the theoretical values of finite element model. The bearing capacity increased by 15%, and coefficient of correction increased by 18%. After the strengthening of the deteriorated bridge, the measured strain values under static loading tests at each span are all less than the values of the bridge before strengthening. The bridge structure showed significant improvement entirely on stiffness as well as bearing capacity. Therefore, the external prestressing reinforcement method not only can effectively improve the structural performance of the bridge, but also can improve the strength and the safety reserve of the bridge.

## CONCLUSION

The deteriorated rigid frame bridge is reinforced by post-tension and steel plate NSM strengthening method, through the comparison and analysis of the measured data of static load test and the calculated data of finite element model, it can be seen that both deflection and strain values of control section decreased after bridge strengthening compared with the bridge before reinforcement. The bearing capacity, crack resistance and deflection of the rigid frame bridge after reinforcement meet the design requirements. And the bearing capacity, stiffness and safety reserve of the bridge can be improved after reinforcement. The proposed strengthening method has been proved to be effective. It is suggested that low relaxation prestressed steel wire bundles should be selected when strengthening continuous rigid frame bridges. The prestressed steel wire bundle adopts two-end stretching mode and the super-tension can effectively reduce the loss of the prestress. For the crack disease of box girder of continuous rigid frame bridge, it is effective to repair the crack of box girder strengthened with bonded steel plate.

## REFERENCES

- [1] Jose A. Instrumentation system for post-tensioned segmental boxgirder bridges. Master dissertation, Austin: University of Texas, 1991
- [2] Vladimir K, Zdenek P, Milos Z, and Alena K. Box girder bridge deflections, (2006). ACI concrete international, Vol. 28 (1): 55–63
- [3] H. Lee, W. Jung, W. Chung, (2018). Field test of an old RC bridge before and after NSM strengthening. Composite Structures; Vol. 202:793-801
- [4] H. Osman, A. Sreenivas, K. Jonathan, (2001). Application of FRP laminates for strengthening of a reinforced-concrete T-beam bridge structure. Composite Structures 52:453-466.

- [5] Zhang, Kexin , and Q. Sun, (2017). "Experimental Study of Reinforced Concrete T-Beams Strengthened with a Composite of Prestressed Steel Wire Ropes Embedded in Polyurethane Cement (PSWR–PUC)." *International Journal of Civil Engineering*. 16:1109–1123.
- [6] Morris. S, (1978). Survey of the durability performance of posttensioning tendons. *ACI J*, vol. 75(10):501–510.
- [7] J. L. Xu, Z. L. Yi, J. L. Yang, (2013). A Study on the Quality Assessment System of External Prestressing Reinforcement Technology, *Applied Mechanics and Materials*, vol. (351-352): 1347-1353.
- [8] Y. Shen, T.Y. Song, G.P. Li, 2015. Advances of external prestressing tendons in multi-span curved box-girder bridges. *Multi-Span Large Bridges – Proceedings of the International Conference on Multi-Span Large Bridges*, 1255-1262.
- [9] A. M. Ibrahim, (2010). Parametric study of continuous concrete beam Prestressed with external tendon. *Jordan Journal of Civil Engineering*, vol. (4)3:211-221.
- [10] Lopez, A. , Galati, N. , Alkhrdaji, T. , & Nanni, A., 2007. Strengthening of a reinforced concrete bridge with externally bonded steel reinforced polymer (srp). *Composites Part B (Engineering)*, vol. 38(4), 429-436.
- [11] Oh, H. , Sim, J. , & Meyer, C., 2003. Experimental assessment of bridge deck panels strengthened with carbon fiber sheets. *Composites Part B Engineering*, vol. 34(6), 527-538.
- [12] Lee H Y , Jung W T , Chung W,( 2017).Flexural strengthening of reinforced concrete beams with pre-stressed near surface mounted CFRP systems. *Composite Structures*, vol. 163:1-12
- [13] Fathelbab, F. A. , Ramadan, M. S. , & Al-Tantawy, A. . (2014). Strengthening of RC bridge slabs using CFRP sheets. *Alexandria Engineering Journal*, 53(4), 843-854.
- [14] Maléna Bastien-Masse, & Eugen Brühwiler, 2013. Concrete bridge deck slabs strengthened with uhpfrc. *labse Symposium Report*, vol. 99(22).
- [15] Lee H, Jung W T, Chung W, (2017). Post-tension near-surface-mounted strengthening systems of full-scale PSC girders. *Construction and Building Materials*, vol. 151: 71-82.
- [16] Khudeira, S. . (2010). Strengthening of deteriorated concrete bridge girders using an external posttensioning system. *Practice Periodical on Structural Design and Construction*, 15(4), 242-247.
- [17] Parke G A , Disney P , Ahmadikashani K, (2005).Strengthening box-girder bridges using external post-tensioning. *Thomas Telford*:97-104.
- [18] Dunker, K. F. . (1985). Strengthening of simple span composite bridges by post-tensioning.
- [19] Van Lier, J. , & Pronk, M. . (2013). Reinforcing concrete box girder bridges with external post-tensioning and steel. *IABSE Symposium Report*, 99(22), 670-677.
- [20] Taljsten, B. , & Nordin, H. . (2007). Concrete beams strengthened with external prestressing using external tendons and near-surface-mounted reinforcement (nsmr). *Journal of Quantitative Spectroscopy & Radiative Transfer*.
- [21] JTG D60-2004 General Code for Design OF Highway Bridges and Culverts. P.R. China, Ministry of Communications, 2004.
- [22] JTJ 021-1989. General Code for Design of Highway Bridges and Culverts, P.R. China, Ministry of Communications,1989.
- [23] AASHTO LRFD bridge design specifications, third edition. Washington, DC: American Association of State Highway and Transportation Officials; 2012.